IOP Conf. Series: Materials Science and Engineering **433** (2018) 012043 doi:10.1088/1757-899X/433/1/012043

Theoretical formulation and numerical simulation of thermal performance enhancements for cascade thermal energy storage systems

Hiba A Hasan[1] and Ihsan Y Hussain[1*]
[1]University of Baghdad /College of Engineering-Mech. Engr. Dept., Baghdad, Iraq
[*]dr.ihsanyahya1@gmail.com, drihsan@uobaghdad.edu.iq

Abstract: Cascaded Thermal Energy Storage (CTES), a term that refers to a thermal energy storage system with multiple phase chance materials (PCMs), has been suggested as a solution for heat transfer reduction through the process of heat exchange by reducing temperature differences. The PCMs used are thus paraffin waxes with different melting temperatures. A numerical simulation was made to determine the optimum length of a CTES system compared with use of a single PCM. The enthalpy-porosity theory was utilised to simulate the phase transition of the PCM, and the simulations then used to mimic the charging and discharging of thermal energy storage of optimum length at different heat transfer fluid flow rates. The results indicated that heat transfer can be greatly enhanced, and melting and solidification time significantly reduced, by using multiple PCMs as compared with using a single PCM.

1. Introduction

In recent years, energy consumption has expanded dramatically because of global economic development. As a result, there has also been an increase in greenhouse gases emission and environmental pollution. These factors have led to increased efforts improve energy efficiency so as to reduce overall energy consumption. Thermal energy storage (TES) is an effective method of balancing energy demand and energy supply, allowing the energy system to be more stable and efficient by storing excess thermal energy during high production hours and using it during low production hours [1].

TES can be categorized into three main divisions: storage of sensible heat, storage of latent heat, and storage of thermochemical energy [2]. Storage of latent heat is an attractive technique due to its ability to supply high density energy storage over a relatively constant temperature range analogous to the phase change temperature of the storage material [3]. The materials used in the storage of latent heat are referred to as phase change materials (PCMs), and such PCMs have been studied in several different applications, including solar power plant energy saving buildings [4], systems of waste heat recovery [5], the cooling of electronic devices [6], greenhouses [7], and solar cookers [8].

During charging, the PCMs absorb heat and their temperatures rise; thus, PCMs perform as sensible storage materials. Solid PCMs thus convert to liquid PCMs and the thermal energy is conveyed in this change. The PCMs absorb thermal energy at even small differences in temperatures and store 5 to 14 times more energy

than sensible storage materials [9]. The process reverses on release of heat during the discharge process and the PCM liquids completely revert into solids.

The high capacity of storage for small temperature differences is the major advantage of latent heat storage over storage of sensible heat; however, this does not mean that storage of latent heat cannot be beneficial at wider temperature differences. Nevertheless, it is reasonable to split a wide temperature difference into smaller divisions, each wrapped in a different PCM with an appropriate phase transition temperature [10]. A combination that uses multiple PCMs with various melting temperatures is called a Cascaded Thermal Energy Storage (CTES) system. Another objective for using CTES is that the charge and discharge time is limited in the most common functional case, and the heat must be released or stored rapidly. During the charging of storage systems with single PCMs, the heat transmits to the PCM from the heat transfer fluid (HTF) very rapidly. Thus, the temperature of the HTF decreases, and the temperature difference between the HTF and the PCM decreases, leading to reduced heat transfer at the storage end. Consequently, the PCM melts quickly at the part where the HTF enters the storage, but very slowly at the storage end where the HTF exits the storage. The problem is the same for discharging: the PCM at the storage ending might not be utilised in raising the HTF's temperature. This problem can be solved by creating a CTES [11].

Farid et al. [12, 13] experimentally and numerically constructed a model that included several cylindrical capsules filled with three PCMs with different melting points; the results showed enhancements in both charging and discharging. Gong and Mujumdar [14, 15] evolved a finite element model for a high-temperature thermal storage system of a slab [15] and a tube [14] that used five PCMs, finding a considerable improvement in heat transfer compared with the use of one PCM. Wang et al. [16] experimentally analysed the charging of a cylindrical thermal storage capsule containing multiple PCMs, discovering that the melting process was 15 to 25% faster than in systems containing one PCM. Shaikh and Lafdi [17] conducted a simulation to study the effects of utilising various arrangements of multiple PCMs slab configurations with various melting points, and they demonstrated significant enhancements in heat transfer. Fang and Chen [18] investigated a shell and tube storage system with multiple PCMs, noting that presence of an optimal assembly of multiple PCMs offered extreme thermal energy charging rates. Wang et al. [19, 20] numerically studied a heat exchange device with a zigzag arrangement including multiple PCMs throughout the discharge [19] and charge [20] process; the results indicated that intensified charging and discharging in comparison with the use of one PCM.

The present paper thus aims to numerically investigate the optimum length of CTES, as compared with a TES with one PCM, and then to perform simulations for charging and discharging CTES with this best length.

2. Physical problem

To determine the optimum length of a CTES, a comparison between Single-stage Thermal Energy Storage (STES) and CTES for different lengths was completed. A STES was formed with only PCM2 (Figure 1), while the CTES was constituted of three PCMs along the flow direction of HTF: PCM 1, 2, and 3 (Figure 2). The PCMs used were paraffin waxes and their thermo-physical properties are recorded in Table 1 [21]. The melting temperature of PCM2 (in STES) has an intermediate value between PCMs 1 and 3, to give comparability between STES and CTES. The HTF is air, and its properties are listed in Table 2 along with other relevant system parameters. The CTES with the best length was then studied with regard to the charging and discharge process. For the charging process, a PCM with a lower melting temperature was positioned at the end of the storage to ensure that the temperature difference between the HTF and PCMs was sufficiently large to ensure melting of all PCMs; this arrangement was inverted during the discharging process, as shown in Figure 3.

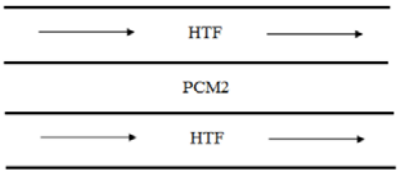

Figure 2. CTES

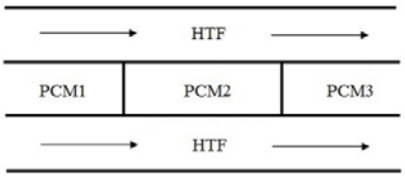

Figure 1. STES

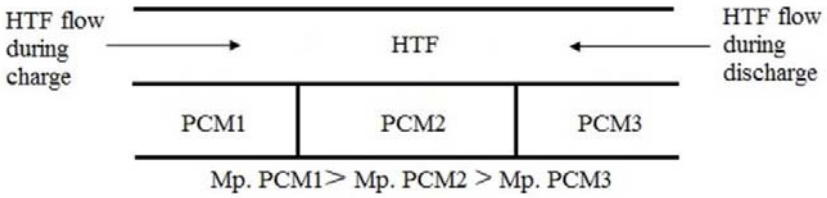

Figure 3. PCM arrangement

Table 1. Thermo-physical properties of PCMs [21]

PCMs	PCM1	PCM2	PCM3
Melting temperature [K]	331	336	340
Solidus Density [kg/m3]	840	850	860
Liquidus Density [kg/m3]	765	766	767
Specific Heat [J/kg K]	2763	2817	2871
Thermal Conductivity [W / m K]	0.21	0.212	0.214
Dynamic Viscosity [kg/m s]	0.0116	0.01215	0.0127
Thermal expansion coefficient [1/K]	0.00031	0.000305	0.0003
Latent Heat [J / kg]	267670	270715	273760
Solidus Temperature [K]	321	326	330
Liquidus Temperature [K]	335	340	344

Table 2. System parameters

HTF properties		System dimensions
Density [kg/m3]	1.225	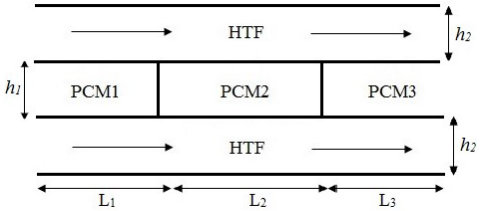
Specific Heat [J/kg K]	1006.43	
Thermal Conductivity [W / m K]	0.0242	
Dynamic Viscosity [kg/m s]	1.7894e-05	
Inlet temperature during charge [K]	373	
Inlet temperature during discharge [K]	294	

h_1 = 20mm, h_2 = 25mm
$L_1 = L_2 = L_3$

3. Numerical model

A simulation of the melting and solidification processes of PCMs was applied using the enthalpy-porosity method [22]. In this method, there is no explicit tracking for the liquid-solid interface; instead, there is a mixed liquid-solid region, referred to as a mushy zone. This zone is modelled as a porous medium, with a porosity specified as equivalent to liquid fraction (β). The value of β is given by [23]

$\beta = 0$ for $T < T_{solidus}$

$\beta = (T - T\_solidus)/(T_{liquidus} - T_{liquidus})$ for $T_{liquidus} < T < T_{solidus}$

$\beta = 1$ for $T > T_{liquidus}$ (1)

where T is the local temperature. Thus, the velocity will be affected as follows:

$V = V_1$ in the liquid phase

$V = \beta V_1$ in the mushy zone

$V = 0$ in the solid phase (2)

where V is the superficial velocity and V_1 is the actual velocity [22]. A Boussinesq approximation is utilised to simulate the natural convection in the PCM, and thus the density of the PCM varies with temperature [24]:

$$\rho = \rho_0 [1 - \gamma(T - T_0)] \quad (3)$$

where ρ is the local density of the PCM, T_0 and ρ_0 are the operating temperature and density, and γ is the thermal expansion coefficient. Assuming the flow of the liquid PCM is Newtonian, incompressible, and laminar, the governing equations are continuity, momentum, and energy. The continuity equation can therefore be illustrated as [25]

$$\frac{\partial \rho}{\partial t} + \nabla.(\rho \vec{V}) = 0 \quad (4)$$

where t is the time. The pressure losses of flow produced by the existence of the solid PCM can be estimated using the source terms in the momentum equation [26]:

$$\rho\left(\frac{\partial \vec{V}}{\partial t} + (\nabla.\vec{V})\vec{V}\right) = \mu(\nabla^2\vec{V}) - \nabla P + \vec{S} \quad (5)$$

where μ is the viscosity of the PCM, p is the pressure, and the vector $\vec{S}$ is a global source term given by the following form:

$$\vec{S} = \frac{(1-\beta)^2}{(\beta^3 + €)^3} A_{mush}\, \vec{V} + \rho \vec{g} \gamma (T - T_0) \quad (6)$$

The first term on the right-hand side appears due to the existence of solid PCM in the mixed region, where € is set as a small number (less than 0.001) to prevent division by zero [27]. A_{mush} is the mushy zone constant, which acts as a damping factor of velocity through the solidification of the PCM. Its value affects the PCM melting rate, and here it is set to 10^5 kg/m^{3}s [28]. The second term is the Boussinesq approximation, which is essential for modelling the natural convection in the liquid phase of the PCM. The vector $\vec{g}$ is the gravitational acceleration, which is equal to 0 m/s^2 in the x-direction and -9.81 m/s^2 in the y-direction. The energy equation can be described as [20]

$$\frac{\partial}{\partial t(\rho h)} + \nabla.\left(\rho\vec{V}h\right) = \nabla.(k\nabla T) + S_h \tag{7}$$

where h is the sensible enthalpy, which can be expressed as [29]

$$h = h_{ref} + \int_{T_{ref}}^{T} C_P dT + \beta L \tag{8}$$

where h_{ref} is the enthalpy at the reference temperature T_{ref}, and C_P and L are the specific heat at a constant pressure and the latent heat of the PCM. S_h is the energy source term, given by [20]

$$S_h = \frac{\partial(\rho\Delta h)}{\partial t} + \nabla.\left(\rho\vec{V}\Delta h\right) \tag{9}$$

The flow of HTF is assumed to be turbulent flow; to consider the turbulence effect, the $(K-\varepsilon)$ model [28] was thus implemented in the numerical model. Two-dimensional numerical simulations were made with ANSYS Fluent. For the grid independence solution, three different grid densities were tested, with 21,600, 84,000, and 336,000 elements, respectively. The results showed that the 84,000 elements density was most suitable, because it represented the best compromise between solution accuracy and computational cost (see Figure 4). A comparison with the work in [30] was undertaken for model validation: the same characteristics were used, and the two models gave similar results (see Figure 5), demonstrating good agreement between them.

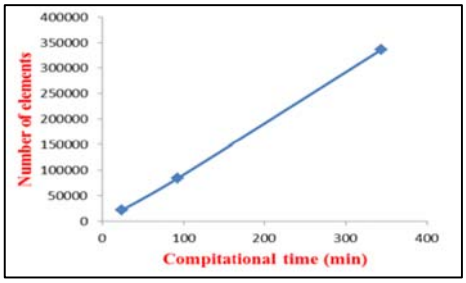

Figure 4. The grid independence solution.

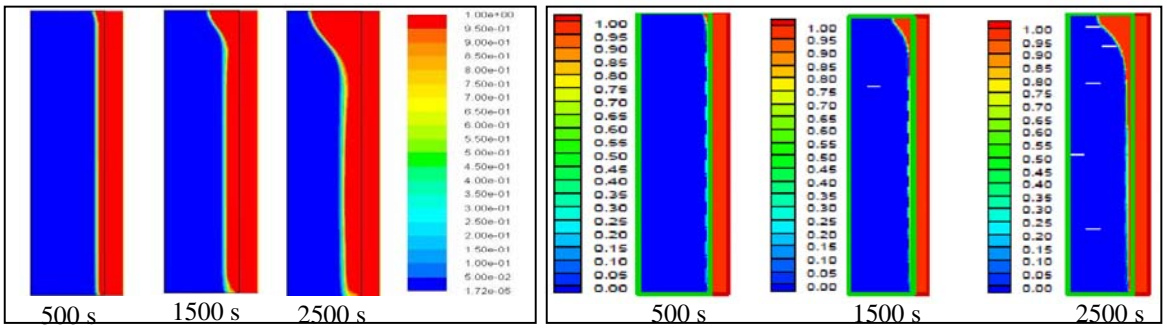

(a) (b)

Figure 5. Comparison between (a) proposed numerical model, and (b) the work in [30]

4. Results and discussion

4.1. Best length of CTES

In order to determine the best length of CTES containing the selected PCMs, a comparison between the CTES and STES was carried out for different lengths (750; 1,000; 1,200; 1,500; and 2,000 mm) during the discharge process. Figure 6 illustrates the percentage of improvement in solidification time of each CTES over STES, categorised by length. As shown, increases in length lead to increases in the percentage of improvement in solidification time to a length of 1,200 mm, where the highest increase in the percentage of improvement is seen; after that, the percentage of improvement decreases. This means that a length of 1,200 mm is optimal for using these PCMs.

Figure 6. The best length of CTES.

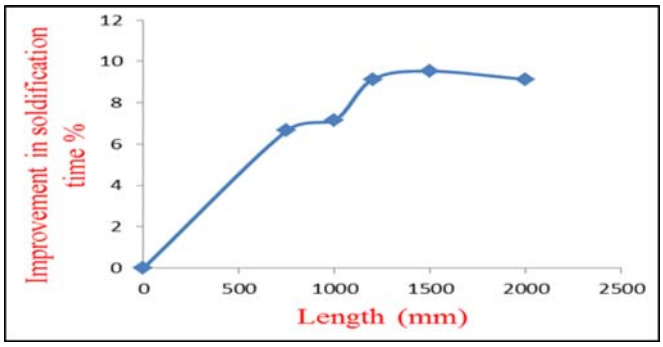

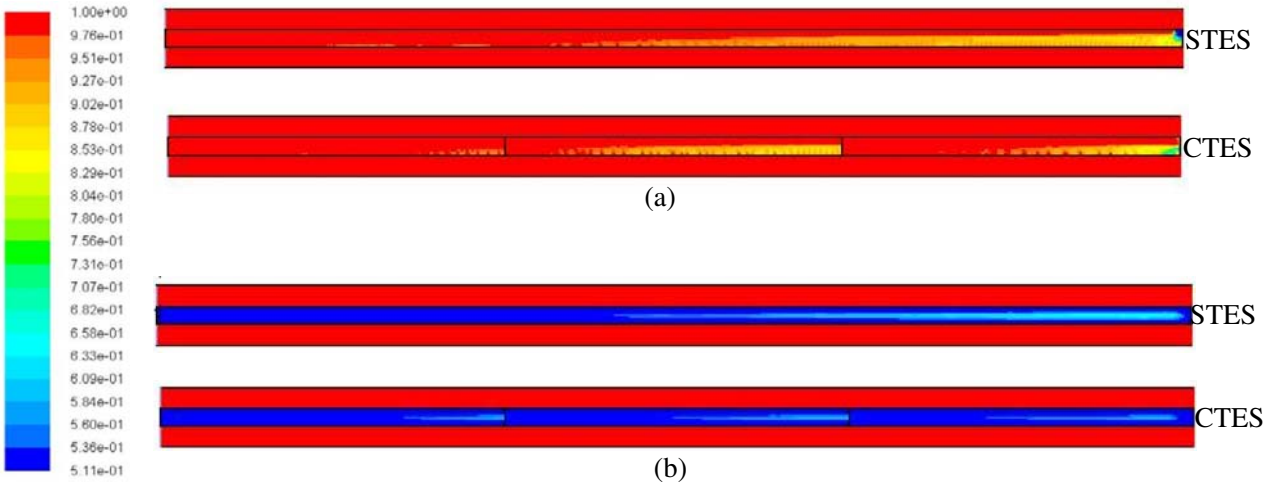

Figure 7. Liquid fraction contour for STES and CTES at 4,000 s for (a) charging and (b) discharging process

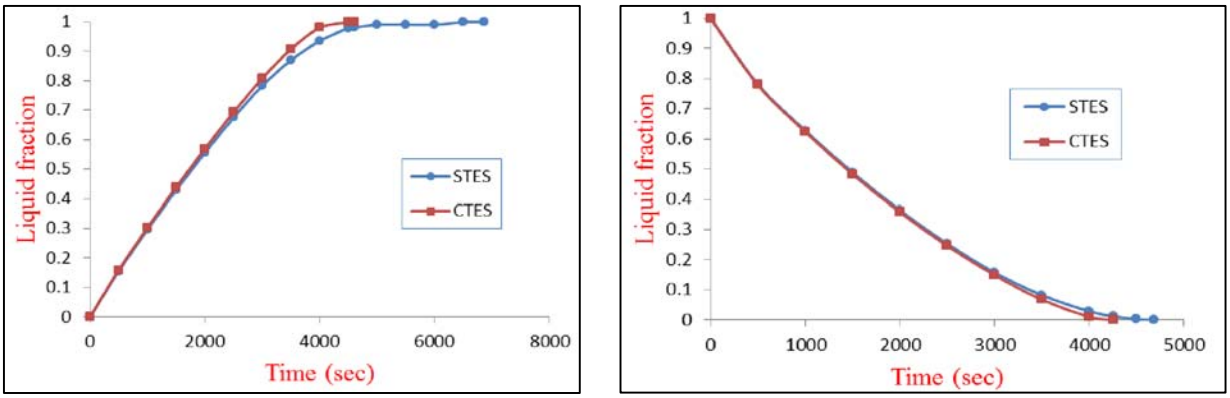

(a) **(b)**

Figure 8. Average liquid fraction for STES and CTES for (a) charging and (b) discharging process.

In Figure 7, the liquid fraction contours for both STES and CTES at the best length can be seen at the same instant of time (4,000 s), for both charging and discharging processes. The red region is the liquid phase, while the blue region is the solid phase. Alternating colours represent the mushy zone. Clearly, the charging and discharging processes are faster and more uniform in CTES compared with STES, as CTES ensures

almost uniform temperature difference between the HTF and PCMs along the storage. Figure 8 also shows a comparison of the average liquid fractions; it can be seen that the liquid fraction tends to rise faster with CTES during the charging process (Figure 8 (a)), where the melting time for STES is 6,860 s, while for CTES it is 4,595 s. Similarly, for the discharge process (Figure 8 (b)), the solidification time for STES was 4,685 s, while for CTES it was 4,257 s. This means that CTES significantly improves heat transfer for both charging and discharging processes, although more improvement is seen for charging process. This finding is critical, and common in all literature dealing with this subject. The main cause of this phenomenon is that during the discharging process, the upper layers of the PCM solidify first, and thus act as additional resistance to heat transfer, reducing any enhancement. However, in the charging process, the upper layers of the PCM melt first, enhancing the heat transfer and allowing natural currents to be developed. As shown in Fig. 8, the effect of CTES is clearly shown in the final stages of the charging and discharging processes; this is because the temperature difference between the PCM and HTF reduces at the final stages in STES, while CTES works to increase this difference and accelerate heat exchange.

4.2. Influence of HTF velocity variation on CTES

The influence of HTF velocity variation on outlet air temperature for the charging and discharging processes is illustrated in Figure 9. During the charging process (Figure 9 (a)), the minimal HTF velocity (v=1 m/s) was used to give the minimal outlet temperature and maximum difference between inlet and outlet temperatures; this is because at lower velocity, the air has more time to flow over the PCMs and enable more heat exchange. The maximum HTF velocity (v=15 m/s) similarly gives the maximum outlet temperature, ensuring minimal difference between inlet and outlet temperatures due to the lower amount of time that the passing air is exposed to PCMs. For the discharging process (Figure 9 (b)), the maximum velocity again gave a minimal difference between outlet and inlet temperatures, and the minimal velocity give the minimal difference between outlet and inlet temperatures, for the reasons mentioned above. Each curve ends when melting (Figure 9 (a)) or solidification (Figure 9 (b)) is complete; this indicates that the HTF velocity affects the melting and solidification time, as shown in Figure 10, where it is noted that increased velocity leads to a significant reduction in both melting and solidification time. It should be noted that the melting process at (v=1 m/s) is never completed; this velocity is not sufficient to melt the PCMs, and thus higher velocities were used throughout.

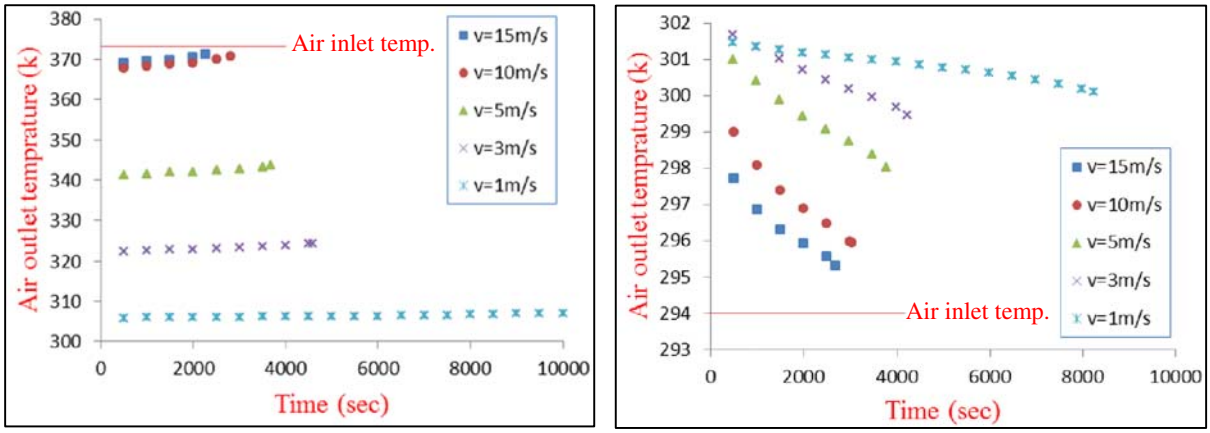

Figure 9. The influence of HTF velocity variation on outlet air temperature for (a) charging and (b) discharging process.

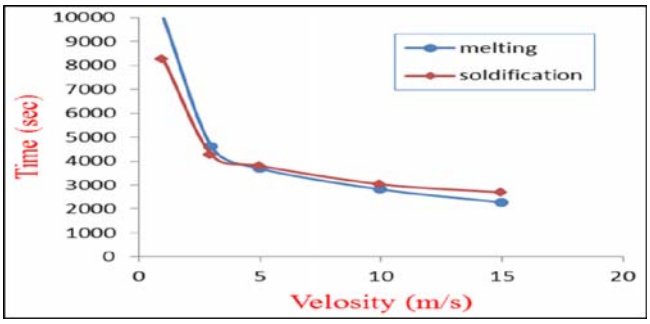

Figure 10. The influence of HTF velocity variation on melting and solidification time.

5. Conclusions

The numerical investigation into thermal performance of CTES was accomplished; the enthalpy-porosity theory was applied to simulate the phase change of the PCMs, and the comparison between STES and CTES for different lengths was established, with the results indicating that the length of CTES was 1,200 mm for the selected PCMs. The CTES with the best length was seen to be greatly enhanced in terms of heat transfer for both charging and discharging processes, especially in the final stage, and the melting and solidification times were significantly reduced. Simulations of the charging and discharging processes for a CTES with the best length under the influence of HTF velocity variations of outlet air temperature were accomplished, and the effects on the melting and solidification times were studied. The results showed that increased velocity reduced the difference between air inlet and outlet temperatures, thus reducing the process time.

References

[1] Mallow A 2015 *Stable paraffin composites for latent Heat thermal storage systems* M.Sc. Thesis (Georgia Institute of Technology).

[2] Chiu J, 2013 *latent heat thermal energy storage for indoor comfort control* Ph.D. Thesis (KTH School of Industrial Engineering and Management).

[3] Sharma S and Sagara K 2005 Latent Heat Storage Materials and Systems: A Review *Int. J. Green Energy* ed Taylor and Francis **2** 1–56.

[4] Tyagi V and Buddhi D 2007 PCM storage in building: a state of art *J. Renewable and Sustainable Energy Reviews* **11** 1146-1166.

[5] Alhamdo M, Theeb M and Golam A 2015 Finned double-tube PCM system as a waste heat storage *IOP Conf. Series: Materials Science and Engineering* vol 95 012033.

[6] Alshaer W, Nada S, Rady M, Barrio E and Sommier A 2015 thermal management of electronic devices using carbon foam and PCM/nano-composite *Int. J. Thermal Sciences* **89** 79-86.

[7] Liu Y, Chen C, Guo H and Yue H 2006 An Application of Phase Change Technology in a Greenhouse *Proceedings of the 6th Int. Conf. for Enhanced Building Operations* (Shenzhen: China) Vol II-2-5.

[8] Saxena A, Lath S and Tirth V 2013 Solar Cooking by Using PCM as a Thermal Heat Storage *MIT Int. J. Mechanical Eng.* **3** 91–95.

[9] Liu Z, Yao Y and Wu H 2013 Numerical phenomena in porous media: shell-and-tube type latent heat thermal energy storage *J. Appl. Energy* **112** 1222–1232

[10] Nakhla D 2013 *An enhanced latent heat thermal storage system using electrohydrodynamics (EHD)* M.Sc. Thesis (McMaster University Hamilton, Canada)

[11] Tian Y 2012 *Heat transfer enhancement in phase change materials (PCMs) by metal foams and cascaded thermal energy storage* Ph.D. Thesis (University of Warwick).

[12] Farid M and Kansawa A 1989 Thermal Performance of a Heat Storage Module Using PCM's With Different Melting Temperature: Experimental *J. Solar Energy Eng.* **112** 125-131.

[13] Farid M and Kansawa A1990 Thermal Performance of a Heat Storage Module Using PCM's With Different Melting Temperature: Mathematical Modeling *J. Solar Energy Eng.* **111** 152-157.

[14] Gong Z and Mujumdar A 1996 Cyclic heat transfer in a novel storage unit of multiple phase change Materials *J. Appl. Thermal Eng.* **16** 807-815.

[15] Gong Z and Mujumdar A 1996 Enhancement of energy charging-discharging rates in composite of different phase change materials *Int. J. Heat Mass Transfer* **39** 725-733.

[16] Wang J, Ouyang Y and Chen G 2001 Experimental study on charging processes of a cylindrical heat storage capsule employing multiple-phase-change materials *Int. J. Energy Res.* **25** 439-447.

[17] Shaikh S and Lafdi K 2006 Effect of multiple phase change materials (PCMs) slab configurations on thermal energy storage *J. Energy Conversion and Management* **47** 2103–2117.

[18] Fang M and Chen G 2007 Effect of different multiple PCMs on the performance of latent thermal energy storage system *J. Appl. Thermal Eng.* **27** 994 -1000.

[19] Wang P, Li D, Huang Y, Zheng X, Wang Y, Peng Z and Ding Y 2016 Numerical Study of Solidification in a Plate Heat Exchange Device with a Zigzag Configuration Containing Multiple Phase- Change-Materials *J. Energies* **9** 394.

[20] Wang P, Li D, Huang Y, Zheng X, Peng Z and Ding Y 2015 Thermal energy charging behavior of a heat exchange device with a zigzag plate configuration containing multi-phase-change-material *J.Appl. Thermal Eng.* **142** 328-336.

[21] Rubitherm Technologies GmBH, Germany (http://www.rubitherm.de).

[22] Voller V and Prakash C 1987 A fixed grid numerical modeling methodology for convection-diffusion mushy region phase-change problems *Int. J. Heat Mass Transfer* **30** 1709-1719.

[23] Hesaraki A 2011 *CFD Modeling of heat charging process in a direct-contact container for mobilized thermal energy storage* Thesis (Malardalen University, Sweden).

[24] Buonomo B, Ercole D, Manca O and Nardini S 2016 Thermal Behaviors of Latent Thermal Energy Storage System with PCM and Aluminum Foam *Int. J. heat and technology* **34** S359-S364.

[25] Saraswat A, Verma A, Khandekar S and Das M 2015 Latent haet thermal energy storage in a heated semi-cylinder cavity: experimental results and numerical validation *Proceedings of the 23rd National Heat and Mass Transfer Conf.* (Thiruvananthapuram: India) Paper No. IHMTC2015- 862.

[26] Buonomo B, Ercole D, Manca O and Nardini S 2016 Numerical simulation of thermal energy storage

with phase change materials in aluminum foam *CLIMA - proceedings of the 12th REHVA World Congress* (University of Naples II, Via Rome No. 29, 81031, Aversa (CE), Italy) vol 4.

[27] Nithyanandam K and Pitchumani R 2014 Computational Studies on Metal Foam and Heat Pipe Enhanced Latent Thermal Energy Storage *J. Heat Transfer* **136** 051503-1

[28] ANSYS FLUENT Theory Guide, 2013.

[29] Sciacovelli A, Colella F and Verda V 2012 Melting of PCF in thermal energy storage unit: Numerical investigation and effect of nanoparticle enhancement *Int. J. Energy Research* pp 1610-1623 - ISSN 0363- 907X

[30] Guo C， Zhang W and Wang D 2014 Numerical investigations of heat transfer enhancement in a latent heat storage exchanger with paraffin/graphite foam *10th Int. Conf. on Heat Transfer, Fluid Mechanics and Thermodynamics* (Orlando: Florida) pp 415-420.